ChemComm

Chemical Communications

www.rsc.org/chemcomm

Number 29 | 7 August 2008 | Pages 3321–3452

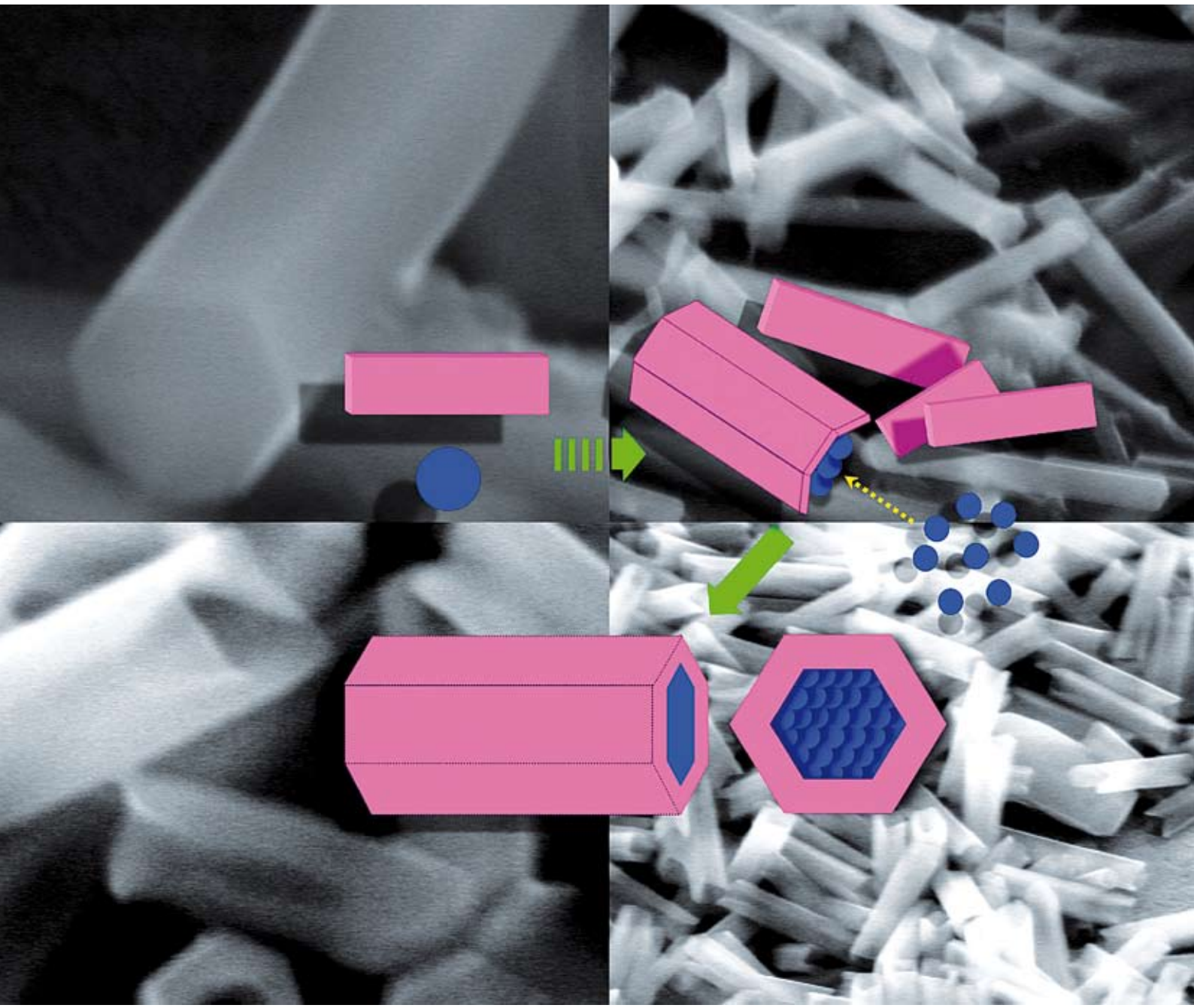

ISSN 1359-7345

COMMUNICATION
Taku Hasobe,
Atula S. D. Sandanayaka *et al.*
Fullerene-encapsulated porphyrin hexagonal nanorods

FEATURE ARTICLE
Roger A. Sheldon
E factors, green chemistry and catalysis: an odyssey

RSC Publishing

Fullerene-encapsulated porphyrin hexagonal nanorods. An anisotropic donor–acceptor composite for efficient photoinduced electron transfer and light energy conversion†

Taku Hasobe,*[ab] Atula S. D. Sandanayaka,*[a] Takehiko Wada[c] and Yasuyuki Araki[c]

Received (in Cambridge, UK) 21st April 2008, Accepted 28th May 2008
First published as an Advance Article on the web 1st July 2008
DOI: 10.1039/b806748a

We have successfully constructed fullerene-encapsulated porphyrin hexagonal nanorods in DMF–acetonitrile solution mixed with CTAB surfactant, which demonstrate efficient and characteristic photoinduced electron transfer and light energy conversion properties.

Construction of functional molecular assemblies with well-defined shapes and structures is of great interest because of a variety of applications such as optoelectronics.[1] Porphyrins are major and promising building blocks for such organized nanoscale superstructures,[2] which perform many of the essential light-harvesting and photoinduced electron/energy transfer reactions.[3,4] Unidirectionally bar-shaped nanostructures of porphyrins (*i.e.* porphyrin nanorods and nanotubes) also have potential for fabrication of nanoscale materials, electronics and photonics because of the characteristic anisotropic structures.[5] However, little attention has been given to the utilization of such structures in electronic and optical applications.[5b]

Fullerenes incidentally hold great promise as spherical electron acceptors on account of their small reorganization energy in electron transfer reactions.[4,6] Combination of porphyrins and fullerenes seems ideal for achieving an enhanced light-harvesting efficiency of chromophores throughout the solar spectrum and a highly efficient conversion of the harvested light into the high energy state of the charge separation by photoinduced electron transfer (PET).[4,6]

Here we report a new type of molecular composites: fullerene-encapsulated porphyrin hexagonal nanorods composed of zinc *meso*-tetra(4-pyridyl)porphyrin [$ZnP(Py)_4$] and C_{60} [denoted as C_{60}-$ZnP(Py)_4$ nanorod], which are prepared with the aid of a surfactant, cetyltrimethylammonium bromide (CTAB), in a DMF–acetonitrile mixed solvent (Fig. 1). The highly organized C_{60}-$ZnP(Py)_4$ nanorods demonstrate not only a broad absorption derived from the supramolecular aggregates, but also significant enhancement of solar energy conversion based on photoinduced charge separation (CS) yielding the radical ion pair [$C_{60}^{\bullet -}$–$ZnP(Py)_4^{\bullet +}$].

[a] *School of Materials Science, Japan Advanced Institute of Science and Technology, Nomi, Ishikawa, 923-1292, Japan. E-mail: t-hasobe@jaist.ac.jp*
[b] *PRESTO, Japan Science and Technology Agency (JST), 4-1-8 Honcho, Kawaguchi, Saitama, Japan*
[c] *Institute of Multidisciplinary Research for Advanced Materials, Tohoku University, Katahira, Sendai, 980-8577, Japan*

† Electronic supplementary information (ESI) available: Experimental part, length distributions, SEM images, XRD measurement, fluorescence lifetime, transient absorption spectroscopy. See DOI: 10.1039/b806748a

$ZnP(Py)_4$ (Aldrich) was purified by recrystallization before use. C_{60}-$ZnP(Py)_4$ nanorods were prepared as follows (Fig. 1).

A mixture of the appropriate ratio of $ZnP(Py)_4$ and C_{60} in DMF solution (1. *Basic monomers*) was injected into 7.5 times volume of continuously stirred 0.20 mM CTAB acetonitrile solution at room temperature. The final concentrations of $ZnP(Py)_4$ and C_{60} are 0.03 and 0.02 mM in DMF–acetonitrile (2/15, v/v), respectively. On injection, they largely form $ZnP(Py)_4$ flake assemblies and C_{60}-based nanoparticles (*ca.* 5–20 nm in diameter), separately (2. *Building Blocks* and Fig. 1A).[7] With the diffusion of DMF into acetonitrile, the Zn–N axial coordination of pyridyl N-atoms to zinc atoms of $ZnP(Py)_4$ promotes the growth of aggregates, which continue to grow into a flake structure.[5c] In this case, the organization process of $ZnP(Py)_4$ moieties is derived from a coordination bond in contrast with C_{60} assemblies based on relatively weak π–π interactions. Therefore, once the components are injected, two different types of assemblies are quickly observed. Fig. 1B shows the build-up of $ZnP(Py)_4$ and C_{60} after 3 min (3. *Built-Up Process*).[7] Then, after several minutes, C_{60}-$ZnP(Py)_4$ nanorods are finally formed (Fig. 1C). The reference $ZnP(Py)_4$ hexagonal nanotube without C_{60} was also prepared in the same manner for comparison [denoted as $ZnP(Py)_4$ nanotube]. It should be noted that the prepared samples were centrifuged at 14 000 rpm to remove CTAB by DMF–acetonitrile solvent repeatedly and filtrated to separate unbound $ZnP(Py)_4$ and

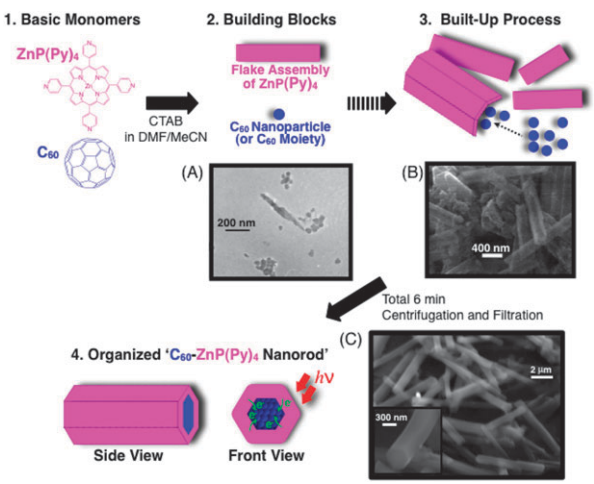

Fig. 1 Schematic illustration of organization process of C_{60} and $ZnP(Py)_4$ using CTAB in this study. CTAB is omitted for clarity. The electron micrographs show the time-dependent formation: (A) 1 min, (B) 3 min and (C) 6 min after injection.

C_{60}. The self-assembled structures can be maintained for many hours. $ZnP(Py)_4$ nanotube shows a bar-like structure with a large hollow hole [see ESI: Fig. S1A†],[5c] whereas the hole is completely closed in C_{60}-$ZnP(Py)_4$ nanorods (Fig. 1C). SEM analysis showed that C_{60}-$ZnP(Py)_4$ nanorods are 4.12 ± 0.94 μm in length and 490 ± 90 nm in outside diameter (Fig. S2†),[8] as compared to $ZnP(Py)_4$ nanotubes analyzed as 2.13 ± 0.27 μm in length and 540 ± 30 nm in outside diameter (Fig. S2†). The large increase in length from 2.13 to 4.12 μm relative to unchanged diameters (~500 nm) indicates that anisotropic crystal growth largely occurs toward the length direction due to π–π interaction of encapsulated C_{60} moieties within the $ZnP(Py)_4$ assembly.[9–11]

To examine electronic interaction in nanorod structures, we have measured steady-state absorption spectra of C_{60}-$ZnP(Py)_4$ nanorod in DMF–acetonitrile (2/15, v/v) (Fig. 2). In the measurement of absorption spectra, we employed an integrating sphere to avoid a scattering effect on the apparent absorption. The absorption spectrum of C_{60}-$ZnP(Py)_4$ nanorod exhibits much broader and more intense absorption in the visible and near infrared regions than those of the corresponding monomers: $ZnP(Py)_4$ or C_{60} in DMF (spectra *b* and *c*). Additionally, the absorption spectrum of C_{60}-$ZnP(Py)_4$ nanorod also becomes broader than that of $ZnP(Py)_4$ nanotube because of aggregated interactions of C_{60} assemblies or C_{60}-$ZnP(Py)_4$ interfaces (Fig. S4†). A quite broad absorption in the visible region is useful for solar energy conversion.

The singlet excited-state quenching of $ZnP(Py)_4$ by encapsulated C_{60} in C_{60}-$ZnP(Py)_4$ nanorods was investigated to obtain the overall fluorescence intensity quenching behavior with respect to the reference $ZnP(Py)_4$ nanotubes (Fig. 3). In steady-state fluorescence measurements, the fluorescence intensity of the porphyrin in C_{60}-$ZnP(Py)_4$ nanorod (spectrum *a*) is suppressed compared to that of the $ZnP(Py)_4$ nanotubes (spectrum *b*). This quenching is largely because of efficient PET from $^1ZnP(Py)_4$* to C_{60} in nanorods.[4] Furthermore, additional quantitative electronic interplay on the photoexcited C_{60}-$ZnP(Py)_4$ nanorods could be evaluated by time resolved fluorescence spectroscopy. The insert of Fig. 3 shows the fluorescence decay profiles of C_{60}-$ZnP(Py)_4$ nanorods, $ZnP(Py)_4$ nanotubes and $ZnP(Py)_4$ monomer, respectively. The fluorescence emission decay of C_{60}-$ZnP(Py)_4$ nanorods (trace *a*) was found to proceed faster than that observed for the $ZnP(Py)_4$ nanotubes (trace *b*)

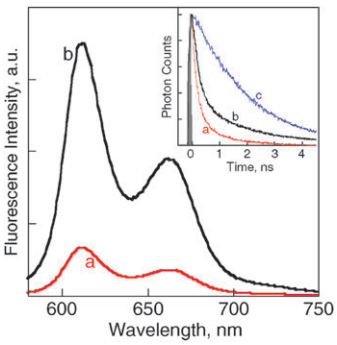

Fig. 3 Steady-state fluorescence spectra of (a) C_{60}-$ZnP(Py)_4$ nanorods and (b) $ZnP(Py)_4$ nanotubes in DMF–acetonitrile = 2/15, v/v. Inset: time-resolved fluorescence decays: (a) C_{60}-$ZnP(Py)_4$ nanorods, (b) $ZnP(Py)_4$ nanotubes and (c) 5 μM $ZnP(Py)_4$ monomer in DMF. λ_{ex} = 408 nm.

and monomer (trace *c*). By the biexponential fitting of the fluorescence decay of C_{60}-$ZnP(Py)_4$ nanorods, the fluorescence lifetimes (τ_f) were evaluated to be 180 ps (85%) and 1100 ps (15%), which are considerably shorter than those of $ZnP(Py)_4$ nanotubes [390 ps (65%) and 1870 ps (35%)] and $ZnP(Py)_4$ monomer [2200 ps (100%)]. It is reasonable to assume that a photoinduced CS state [*i.e.* $ZnP(Py)_4^{\bullet+}$ and $C_{60}^{\bullet-}$] occurs in C_{60}-$ZnP(Py)_4$ nanorods. By comparing the τ_f of C_{60}-$ZnP(Py)_4$ nanorod with that of reference $ZnP(Py)_4$ nanotube, the CS rate constant (k_{CS}) in C_{60}-$ZnP(Py)_4$ nanorods was calculated to be 3.0×10^9 s^{-1} (see: Fig. S5†).

Additional support for the above hypothesis comes from complementary transient absorption spectroscopy measurements performed after laser irradiation of C_{60}-$ZnP(Py)_4$ nanorods at 532 nm (Fig. 4). The characteristic features of the triplet–triplet absorption of $ZnP(Py)_4$ are missing in C_{60}-$ZnP(Py)_4$ nanorods, thus suggesting the efficient quenching of the singlet excited state by the C_{60} moiety, which is in sharp contrast with PET *via* $^3ZnP(Py)_4$* in a reference non-organized system: $(C_{60} + ZnP(Py)_4)_n$ (Fig. S5–7†).[8,12] Interestingly, the transient spectra of C_{60}-$ZnP(Py)_4$ nanorods revealed transient bands corresponding to both $C_{60}^{\bullet-}$ at 1080 nm and $ZnP^{\bullet+}$ at 680 nm.[6b] Thus, considering all the above observations, it is reasonable to assume that the decay rates of the transient absorption bands can be attributed to charge recombination (CR), which occurs after the formation of a CS state in

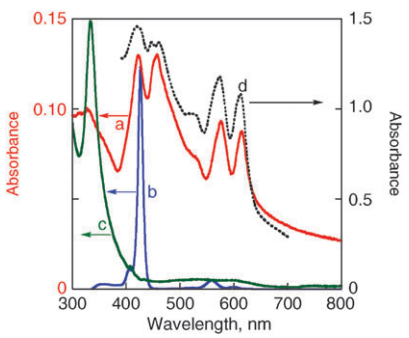

Fig. 2 Steady-state absorption spectra of (a) C_{60}-$ZnP(Py)_4$ nanorods in DMF–acetonitrile (2/15, v/v), (b) 1.3 μM $ZnP(Py)_4$ monomer in DMF, (c) 5 μM C_{60} monomer in DMF and (d) OTE/C_{60}-$ZnP(Py)_4$-nanorod film using an integrating sphere.

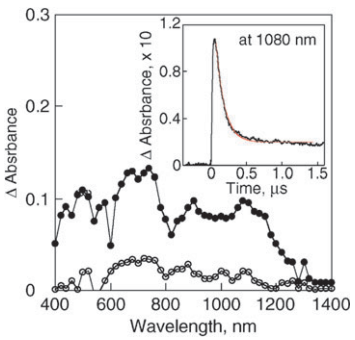

Fig. 4 Nanosecond transient absorption spectra of C_{60}-$ZnP(Py)_4$ nanorods in Ar-saturated DMF–acetonitrile (2/15, v/v) after 532 nm laser irradiation at 0.1 μs (●) and 1.0 μs (○). Inset: the time profiles of $C_{60}^{\bullet-}$ monitored at 1080 nm.

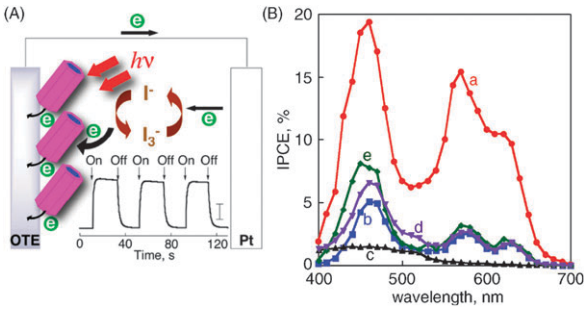

Fig. 5 (A) Illustration of the photoelectrochemical solar cell. The insert shows photocurrent generation responses under white light illumination (AM 1.5). Input power: 82 mW cm^{-2}. The bar is 0.3 mA cm^{-2}. (B) Photocurrent action spectra of (a) OTE/C_{60}-ZnP(Py)$_4$-nanorod, (b) OTE/ZnP(Py)$_4$-nanotube, (c) OTE/C_{60}-assembly, (d) sum of spectra *b* and *c*, and (e) OTE/(ZnP(Py)$_4$ + C_{60})$_n$. Electrolyte: 0.5 mol dm^{-3} LiI and 0.01 mol dm^{-3} I_2 in acetonitrile.

C_{60}-ZnP(Py)$_4$ nanorods. From the decay time profiles of these transient bands, the rate constants of the CR process are calculated to be 1.04×10^7 s^{-1} which corresponds to 100 ns for ZnP(Py)$_4^{\bullet+}$ and $C_{60}^{\bullet-}$.[13] The difference in PET pathways (*i.e.*, *via* excited singlet or triplet state)[12] may have a great effect on light energy conversion properties (*vide infra*).

To evaluate the solar energy conversion properties of C_{60}-ZnP(Py)$_4$ nanorods, we constructed a photoelectrochemical cell composed of C_{60}-ZnP(Py)$_4$ nanorod-modified SnO_2 optically transparent electrode (OTE) [denoted as OTE/C_{60}-ZnP(Py)$_4$-nanorod] by electrophoretic deposition (Fig. 5A).[4]

Fig. 2d shows an absorption spectrum of OTE/C_{60}-ZnP(Py)$_4$-nanorod on an OTE film after deposition, which largely agrees with that in solution. The photocurrent response recorded following the excitation of OTE electrodes is shown in an insert of Fig. 5A. The photocurrent response is prompt, steady and reproducible during repeated on–off cycles of the visible light illumination. Fig. 5B shows photocurrent action spectra of these composite films. The incident photon-to-photocurrent efficiency (IPCE)[4] spectrum of C_{60}-ZnP(Py)$_4$ film (spectrum *a*) shows a broad photoresponse in the visible region (maximum IPCE: ~20% at 460 nm), which parallels the corresponding absorption (spectrum *d* in Fig. 2). In particular, the maximum IPCE value of OTE/C_{60}-ZnP(Py)$_4$-nanorod (~20%: spectrum *a*) is much larger than the sum of two individual IPCE values (spectrum *d*: ~6.5%) of OTE/ZnP(Py)$_4$-nanotube (spectrum *b*) and OTE/C_{60}-assembly (spectrum *c*) under the same conditions. Additionally, the maximum value of OTE/C_{60}-ZnP(Py)$_4$-nanorod (~20%) is much larger than that of a non-organized system: OTE/(ZnP(Py)$_4$ + C_{60})$_n$ (spectrum *e*: ~8%).[8] These results clearly indicate that an organized structure between C_{60} and ZnP(Py)$_4$ as well as the excellent electron acceptor property of C_{60} has a great effect on the light energy conversion property. Such control of an ultrafast PET pathway *via* ^{1}ZnP(Py)$_4$* in a nanorod assembly largely contributes to the improvement of IPCE because of the occurrence of strong fluorescence quenching in a ZnP(Py)$_4$ only assembly (average quenching quantum yield: ~0.8 in Fig. S5†). Photocurrent generation in the present system may be initiated by photoinduced CS from ^{1}ZnP(Py)$_4$* (^{1}ZnP*/ZnP$^{\bullet+}$ = −1.0 V *vs.* NHE)[4] to C_{60} (C_{60}/$C_{60}^{\bullet-}$ = −0.2 V *vs.* NHE)[4] in ZnP(Py)$_4$-C_{60} rather than direct electron injection to a conduction band of SnO_2 (0 V *vs.* NHE).[4] The reduced C_{60} injects electrons into the SnO_2 nanocrystallites, whereas the oxidized porphyrin (ZnP/ZnP$^{\bullet+}$ = 1.0 V *vs.* NHE)[4] undergoes the ET reduction with the iodide ion (I_3^-/I^- = 0.5 V *vs.* NHE).[4]

In summary, we have successfully constructed new fullerene-encapsulated porphyrin hexagonal nanorods prepared in DMF–acetonitrile. These organized assemblies demonstrate controlled PET and efficient solar energy conversion properties. Such systems could pave the way for the development of photoenergy conversion systems.

This work was partially supported by Grants-in-Aid for Scientific Research (No. 19710119 to T.H.) and special coordination funds for promoting science and technology from the Ministry of Education, Culture, Sports, Science and Technology, Japan.

Notes and references

1. (*a*) C. Joachim, J. K. Gimzewski and A. Aviram, *Nature*, 2000, **408**, 541; (*b*) G. M. Whitesides and B. Grzybowski, *Science*, 2002, **295**, 2418.
2. (*a*) P. D. W. Boyd and C. A. Reed, *Acc. Chem. Res.*, 2005, **38**, 235; (*b*) C. M. Drain, G. Smeureanu, S. Patel, X. Gong, J. Garnod and J. Arijeloyea, *New J. Chem.*, 2006, **30**, 1834.
3. D. Kim and A. Osuka, *J. Phys. Chem. A*, 2003, **107**, 8791.
4. T. Hasobe, K. Saito, P. V. Kamat, V. Troiani, H. Qiu, N. Solladié, K. S. Kim, J. K. Park, D. Kim, F. D'Souza and S. Fukuzumi, *J. Mater. Chem.*, 2007, **17**, 4160.
5. (*a*) Z. Wang, C. J. Medforth and J. A. Shelnutt, *J. Am. Chem. Soc.*, 2004, **126**, 16720; (*b*) A. D. Schwab, D. E. Smith, B. Bond-Watts, D. E. Johnston, J. Hone, A. T. Johnson, J. C. dePaula and W. F. Smith, *Nano Lett.*, 2004, **4**, 1261; (*c*) J. S. Hu, Y. G. Guo, H. P. Liang, L. J. Wan and L. Jiang, *J. Am. Chem. Soc.*, 2005, **127**, 17090; (*d*) T. Hasobe, S. Fukuzumi and P. V. Kamat, *J. Am. Chem. Soc.*, 2005, **127**, 11884; (*e*) T. Hasobe, H. Oki, A. S. D. Sandanayaka and H. Murata, *Chem. Commun.*, 2008, 724.
6. (*a*) S. Fukuzumi and H. Imahori, in *Electron Transfer in Chemistry*, ed. V Balzani, Wiley-VCH, Weinheim, 2001, vol. 2, pp. 927–975; (*b*) F. D'Souza, P. M. Smith, M. E. Zandler, A. L. McCarty, M. Itou, Y. Araki and O. Ito, *J. Am. Chem. Soc.*, 2004, **126**, 7898.
7. We cannot exclude the possibility of composite molecular aggregation between ZnP(Py)$_4$ and C_{60} in Fig. 1A and B due to the strong interaction of porphyrins and C_{60} (see: ref. 2*a*). However, definite discrimination is hard since these steps proceed continuously in solution.
8. In the case of preparation of ZnP(Py)$_4$ and C_{60} composite assemblies prepared without CTAB [denoted as (ZnP(Py)$_4$ + C_{60})$_n$], non-uniform rectangular structures are observed. See: Fig. S1B and C†.
9. We have also measured XRD patterns of C_{60}-ZnP(Py)$_4$ nanorods and ZnP(Py)$_4$ nanotubes to examine the internal structures (Fig. S3†). The pattern of C_{60}-ZnP(Py)$_4$ nanorod (pattern *a*) is approximately the same as that of ZnP(Py)$_4$ nanotube (pattern *b*). This suggests that ZnP(Py)$_4$ assemblies in the nanorods have quite similar structures to ZnP(Py)$_4$ nanotube, and C_{60} moieties are encapsulated within the ZnP(Py)$_4$ assemblies as shown in Fig. 1.
10. The crystal structure of ZnP(Py)$_4$ was previously reported. Considering the unit cell structure, the growth direction of the rod-assembly is *c* axis. See: Fig. S3†, ref. 5*c* and H. Krupitsky, Z. Stein, I. Goldberg and C. E. Strouse, *J. Inclusion Phenom. Mol. Recognit. Chem.*, 1994, **18**, 177 and L. Kuan-Jiuh, *Angew. Chem., Int. Ed.*, 1999, **38**, 2730.
11. The final molar ratio between ZnP(Py)$_4$ and C_{60} was determined to be 3 : 1 by absorption measurement.
12. In contrast with C_{60}-ZnP(Py)$_4$ nanorod, PET *via* ^{3}ZnP(Py)$_4$* occurs in (ZnP(Py)$_4$ + C_{60})$_n$. See: Fig. S5–7†.
13. In the inset of Fig. 4, the minor and long lifetime species may be attributable to a migration process of $C_{60}^{\bullet-}$ in the encapsulated C_{60} assembly.

